Supplementary Information (SI) for Polymer Chemistry.
This journal is © The Royal Society of Chemistry 2025

SUPPLEMENTARY INFORMATION

Synthesis of Triamine-Functionalized Rigid Crosslinkers for Material Science

Niccolò Braidi,[1] Aitor Hernández,[2] Giulia Scurani,[1] Francesca Parenti,[1] Nezha Badi[2], Filip E. Du Prez[2]**

[1] Department of Chemical and Geological Sciences, University of Modena and Reggio Emilia, via Campi 103, 41125, Modena, Italy

[2] Polymer Chemistry Research Group, Centre of Macromolecular Chemistry, Department of Organic and Macromolecular Chemistry, Faculty of Sciences, Ghent University, Krijgslaan 281 (S4), 9000 Ghent, Belgium

E-mails: niccolo.braidi2@unibo.it; filip.duprez@ugent.be

1. Materials

The commercial reagents were used as received: styrene (TCI Europe, > 99.0%), copper (II) bromide (Acros Organics, > 99%), 4,4'-dinonyl-2,2'-bipyridine (BLDpharm, 98%), 2,6-dimethylpyridine (TCI Europe, > 98.0%), 1,3,5-tris(bromomethyl)benzene (BLDpharm, 97%), anisole (TCI Europe, > 99.0%), dichloromethane (Fisher Chemical, ≥ 99.8%), methanol (Chemlab, > 99%), tetrahydrofuran stabilized with BHT (Acros Organics, 99.9%), dimethylformamide (Fischer Scientific, 99.7%), bisphenol A diglycidyl ether (Sigma-Aldrich, used as embedding medium), Pripol 2033 was kindly provided by Croda. 5,6-isopropylidene-L-ascorbic acid has been synthesized following a procedure from the literature.[1]

2. Syntheses

2.1 - Synthesis of trisBromoPS

A solution of styrene (20 mL, 175 mmol), anisole (10 mL), and 2,6-dimethylpyridine (150 µL, 1.29 mmol) was bubbled with nitrogen for 30 min. $CuBr_2$ (20 mg, 0.0895 mmol), 4,4'-dinonyl-2,2'-bipyridine (143 mg, 0.350 mmol), 5,6-isopropylidene-L-ascorbic acid (94 mg, 0.435 mmol), and 1,3,5-tris(bromomethyl)benzene were weighed in a Schlenk flask and three vacuum/nitrogen cycles were performed. The solution was introduced in the flask under nitrogen flow. The Schlenk flask was then sealed under nitrogen and put in a preheated oil bath (100 °C). After 14 h of reaction, the orange reaction mixture was diluted with dichloromethane (25 mL) and precipitated in methanol (600 mL). The precipitate was filtered through a filter funnel with sintered glass and washed twice with methanol. After drying the filtrate, the conversion (*p*) and consequently the theoretical number average molar mass were determined by gravimetry (**Equation S1**).

[**S1**] $$M_{\mathrm{n}}^{\mathrm{th}} = \frac{[\mathrm{styrene}]_0}{[\mathrm{initiator}]_0} \cdot \mathrm{MW}_{\mathrm{styrene}} \cdot p + \mathrm{MW}_{\mathrm{initiator}}$$

2.2 - Synthesis of trisAzidePS

The chosen amount of trisBromoPS ($w_{\mathrm{trisBromoPS}}$) was weighted and transferred to a flask together with sodium azide (1.5 eq. with respect to the bromide functionalities) and dimethylformamide ($V_{\mathrm{DMF}} = 6\ (\mathrm{mL} \cdot \mathrm{g}^{-1}) \cdot w_{\mathrm{trisBromoPS}}$). The mixture was stirred in a pre-heated oil bath (30 °C) for 4 h before being precipitated in a solution of methanol (600 mL) and NaOH 1 M (20 mL). The precipitate was filtered through a filter funnel with sintered glass and washed twice with methanol. After drying the filtrate, the *yield* was determined by gravimetry ($\overline{yield}$ = 94.6 ± 2.84%).

2.3 - Synthesis of trisAminoPS

The trisAzidePS ($w_{\text{trisAzidePS}}$) was transferred to a two-neck flask together with tetrahydrofuran ($V_{\text{THF}} = 6\ (\text{mL} \cdot \text{g}^{-1}) \cdot w_{\text{trisAzidePS}}$). A waterless condenser was fitted on the flask and the solution bubbled with nitrogen for 30 min. Tributylphosphine (2 eq. with respect to the azide functionalities) was introduced first and then, once the evolution of nitrogen ceases, water ($V_{\text{H}_2\text{O}} = 0.6\ (\text{mL} \cdot \text{g}^{-1}) \cdot w_{\text{trisAzidePS}}$) was introduced as well. The flask was placed in a preheated oil bath (60 °C). After overnight reaction, the mixture was precipitated in a solution of methanol (600 mL) and NaOH 1 M (20 mL). The precipitate was filtered through a filter funnel with sintered glass and washed twice with methanol. The product was re-dissolved in tetrahydrofuran and the precipitation-filtration step was repeated. After drying the filtrate, the *yield* (**Table S3**) was determined by gravimetry.

2.4 - Synthesis of Pripol 2033 Acetoacetate

The synthesis was adapted from a procedure described in literature.[2] Pripol 2033 (1 eq) and *tert*-butylacetoacetate (2.1 eq) were added to a round-bottom flask. The viscous mixture was heated under a moderate vacuum (from 540 to 100 mbar, 130 °C, 4 h). Once the *tert*-butanol stopped condensing over, the excess *tert*-butylacetoacetate was removed by vacuum distillation (<2 mbar, 130 °C).

2.5 - Synthesis of networks

The trisAminoPS and either bisphenol A diglycidyl ether (BADGE) (in a 1:3 molar ratio) or Pripol 2033 acetoacetate (in a 2.1:3 molar ratio) were added to a glass vial along with a stirring bar. For the vinylogous-urethane networks, toluene ($V_{\text{toluene}} = 1\ (\text{mL} \cdot \text{g}^{-1}) \cdot w_{\text{trisAminoPS}}$) was also added. The vial was then sealed with a septum cap, punctured with a syringe needle. The homogeneous mixture was heated in a heating block at 100 °C overnight. Subsequently, the

resulting gel was dried initially in an oven at 120 °C (overnight) and then in a vacuum oven at 140 °C (overnight).

3. Characterizations

3.1 – Gel Permeation Chromatography (GPC)

Measurements were performed on an Agilent PLGPC 50 plus, 2PLgel 5 mm MIXED-D columns at 40 °C, with a refraction index detector. The standards used for calibration were polystyrene and polymethylmethacrylate. A 5% *v/v* of triethylamine in tetrahydrofuran was used as the eluent (1 mL/min). Samples were injected using a PL-AS RT autosampler. From the obtained molar mass distributions, the unidimensional descriptors could be estimated: number and mass average molar masses (M_n^{GPC} and M_w^{GPC}, respectively) and dispersity ($Đ = M_w^{GPC}/M_n^{GPC}$).

3.2 – Nuclear Magnetic Resonance (NMR) spectroscopy

^{1}H-NMR spectra were recorded on a Bruker Avance II 400 (400 MHz) at 25 °C. $CDCl_3$ was used as solvent. Chemical shifts are presented in parts per million (δ) and calibrated to the characteristic residual $CHCl_3$ signal. The following **Equation S2** and **S3** where used to define the three-arm star molar fraction (χ_{star}) and chain-end functionality (*f*), respectively.

[S2] $$\chi_{\text{star}} = \frac{2\cdot(A_{\text{CH}} - A_{\text{CH}_2})}{A_{\text{CH}_2} + 2\cdot A_{\text{CH}}}$$

[S3] $$f_{NMR} = \frac{18\cdot(A_{\text{CH}_2} + A_{\text{CH}})}{A_{\text{ene}}\cdot(4 - \chi_{\text{star}}) + 6\cdot(A_{\text{CH}_2} + A_{\text{CH}})}$$

Where: A_{CH_2} is the area attributed to the benzylic protons of the primary carbon bearing the functionality of interest, A_{CH} is the area attributed to the benzylic protons on the secondary carbon of the chain-end, and A_{ene} is the area attributed to the two protons on the dehydrohalogenated chain-end. The chemical shifts of these are reported in the main manuscript.

3.3 – Thermogravimetric Analysis (TGA)

TGA were performed on a Mettler Toledo TGA/SDTA851e instrument under air atmosphere at a heating rate of 10 °C/min from 25 °C to 800 °C in dynamic mode. The isothermal thermogravimetric measurements were recorded in an air atmosphere at 225 °C for 120 min.

3.4 – Differential Scanning Calorimetry (DSC)

To determine the glass transition temperature (T_g), DSC were performed on a Mettler Toledo instrument 1/700 under nitrogen atmosphere at a heating and cooling rate of 5 °C/min. Measurements were performed from –20 to 160 °C.

3.5 – Online ATR FT-IR

Time-resolved online ATR FT-IR spectra were recorded on a React-IR 702L Instrument (Mettler Toledo AutoChem ReactIR) with TE MCT detector (thermoelectrically Cooled Mercury Cadmium Telluride detector). The probe interface was an AgX 6 mm x 1.5 m fiber with a DiComp (diamond) probe tip. The probe was introduced into one of the necks of the flask containing the reaction mixture and one spectrum was recorded every minute. The solvent spectrum was recorded at the reaction temperature and subtracted to enhance the signal of the reaction species.

3.6 – Matrix-Assisted Laser Desorption/Ionization Time of Flight (MALDI TOF)

A stock solution of the matrix (trans-2-[3-(4-*tert*-butylphenyl)-2-methyl-2-propenylidene]malonitrile (DCTB), 30 mg/mL) and silver trifluoroacetate (AgTFA, 10 mg/mL) were prepared in tetrahydrofuran. The polymers were solubilized in tetrahydrofuran (10 mg/mL). 45 uL of the matrix solution, 15 uL of the salt, and 15 uL of the sample solution were mixed and spotted on the MALDI plate. After evaporation of the solvent at room temperature, the samples were loaded into an Applied Biosystems Sciex 4800+ MALDI ToF analyzer, controlled by 4000

Series Explorer software (Applied Biosystems, Germany). The instrument was operated in reflective positive ion mode.

3.7 – Reprocessability

The networks were (re)processed using a hydraulic press/compression molding (Carver). The samples were broken into small pieces and then brought into a circular mold for compression molding. All the materials were pressed at 160 °C for 60 min with an applied pressure of 4 metric ton. Homogeneous materials were obtained for all formulations.

3.8 – Solubility tests

Samples weighing 10-20 mg were added to a vial and immersed in 40 mL of tetrahydrofuran for 24 h at room temperature. After weighing the swollen sample, the solvent was removed in a vacuum oven (60 °C) until constant weight. The soluble fraction and swelling ratio were calculated using the following equations:

[**S4**] $$Soluble\ fraction\ (\%) = \frac{m_{initial} - m_{final}}{m_{initial}} \cdot 100$$

[**S5**] $$Swelling\ ratio\ (\%) = \frac{m_{swollen} - m_{final}}{m_{final}} \cdot 100$$

3.9 – Rheological Experiments

Amplitude sweeps and stress-relaxation experiments were performed on an Anton-Paar Physica MCR 302 rheometer with a parallel plate geometry (diameter = 8 mm). Samples had a diameter of 8 mm and thicknesses around 1 mm. Amplitude sweep experiments were performed using a frequency of 1 Hz, a constant normal force of 1 N, and a variable shear strain that was ramped up logarithmically from 0.01 to 10% at 130 °C. Stress-relaxation measurements were performed with a constant 2% strain, a constant normal force of 1 N, in a temperature range from 195 to 160 °C, decreasing the temperature at 5 °C intervals.

4. Additional figures

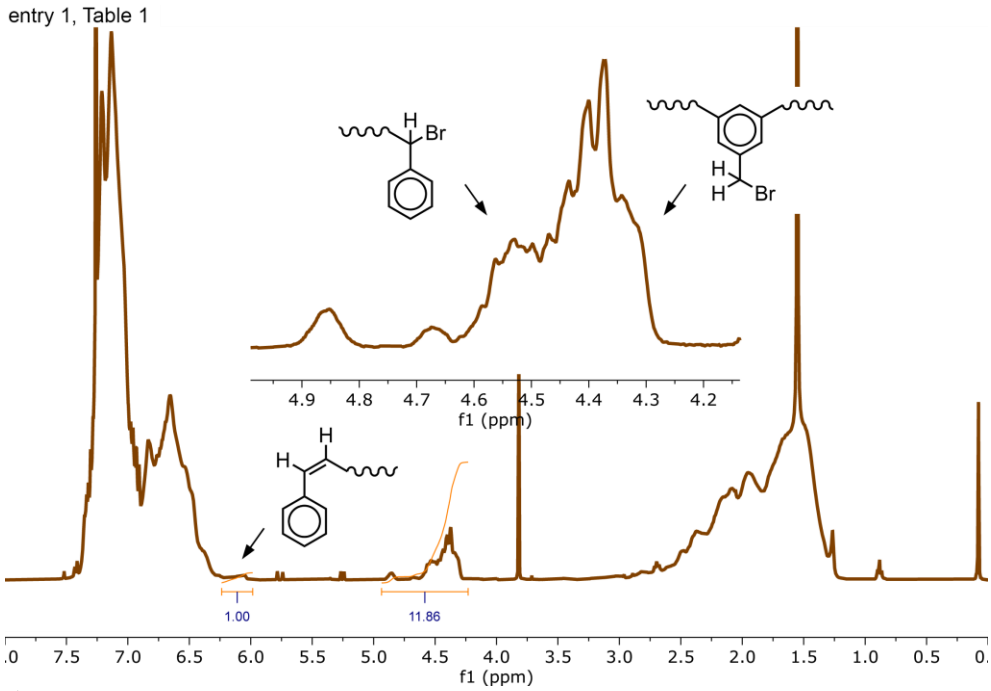

Figure S1. ^{1}H-NMR spectrum of the trisBromoPS reported in **entry 1**, **Table 1**. The inset highlights the proton signals geminal to the bromide functionality. The integration of the above-mentioned signals and of the dehydrohalogenated chain-ends are given in the spectrum.

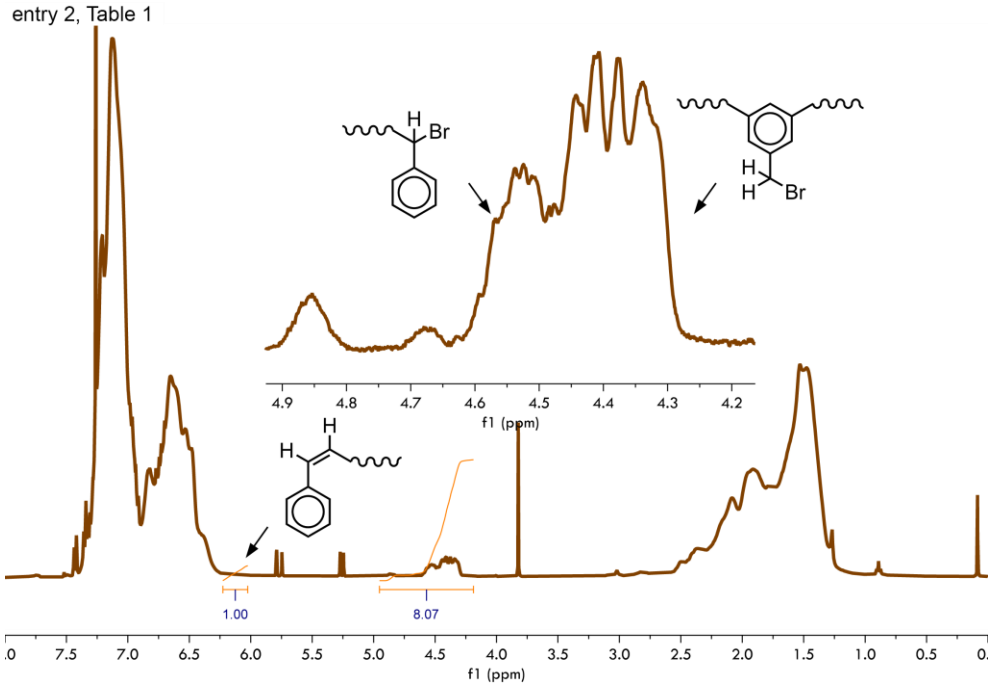

Figure S2. ^{1}H-NMR spectrum of the trisBromoPS reported in **entry 2**, **Table 1**. The inset highlights the proton signals geminal to the bromide functionality. The integration of the above-mentioned signals and of the dehydrohalogenated chain-ends are given in the spectrum.

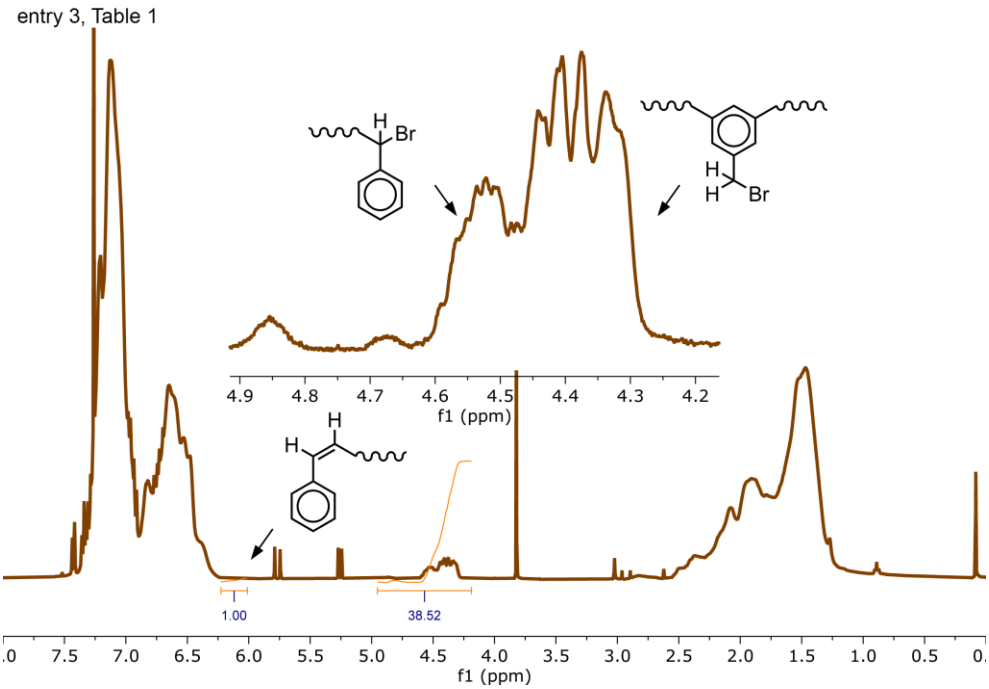

Figure S3. ^{1}H-NMR spectrum of the trisBromoPS reported in **entry 3**, **Table 1**. The inset highlights the proton signals geminal to the bromide functionality. The integration of the above-mentioned signals and of the dehydrohalogenated chain-ends are given in the spectrum.

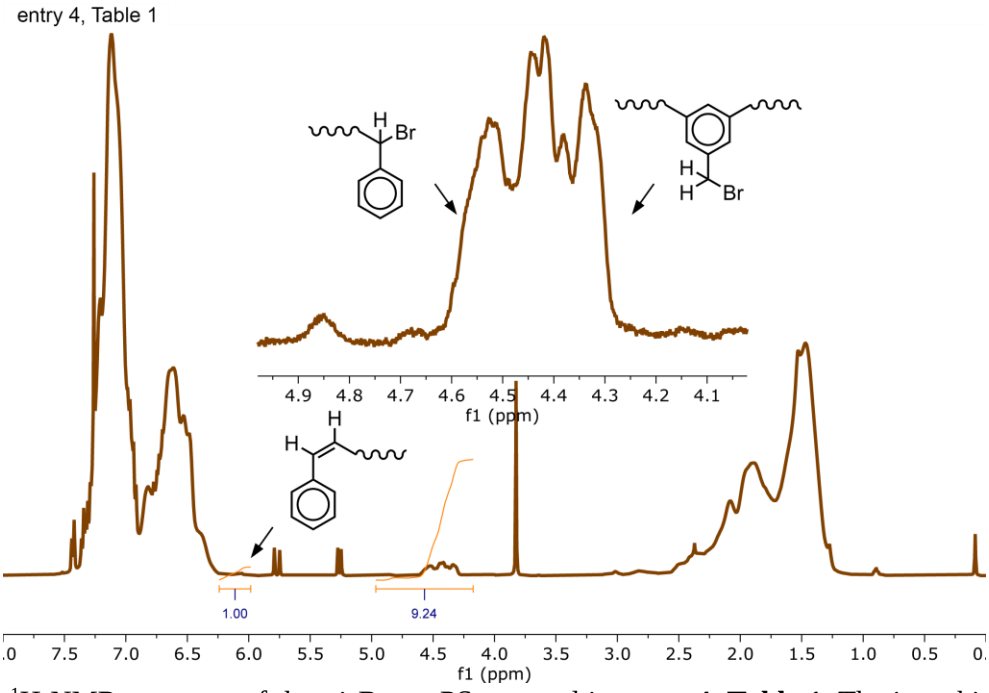

Figure S4. ^{1}H-NMR spectrum of the trisBromoPS reported in **entry 4**, **Table 1**. The inset highlights the proton signals geminal to the bromide functionality. The integration of the above-mentioned signals and of the dehydrohalogenated chain-ends are given in the spectrum.

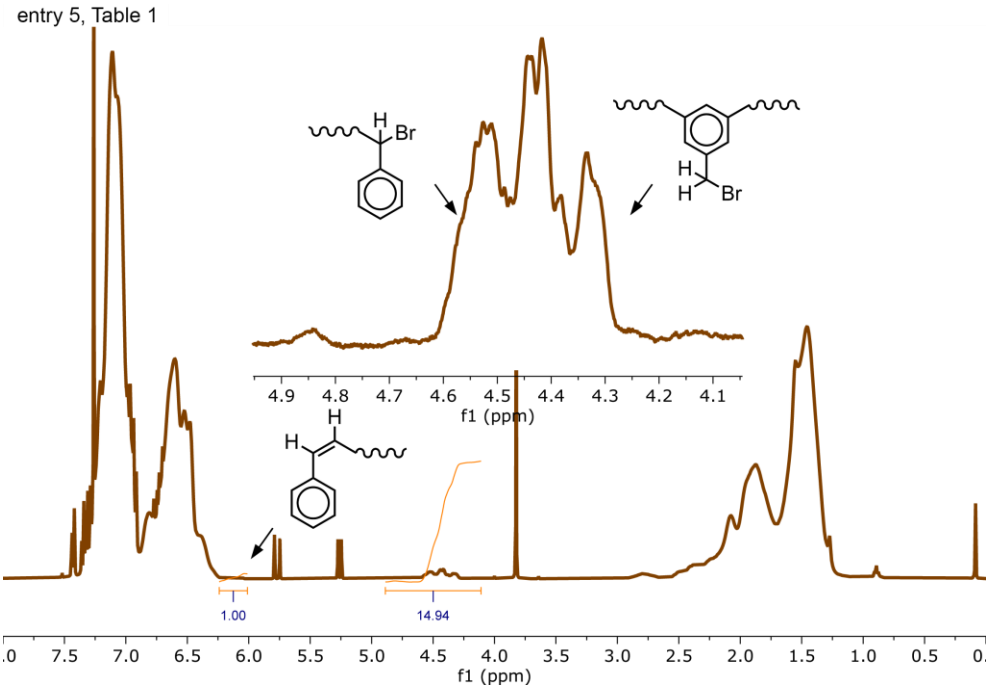

Figure S5. ^{1}H-NMR spectrum of the trisBromoPS reported in **entry 5**, **Table 1**. The inset highlights the proton signals geminal to the bromide functionality. The integration of the above-mentioned signals and of the dehydrohalogenated chain-ends are given in the spectrum.

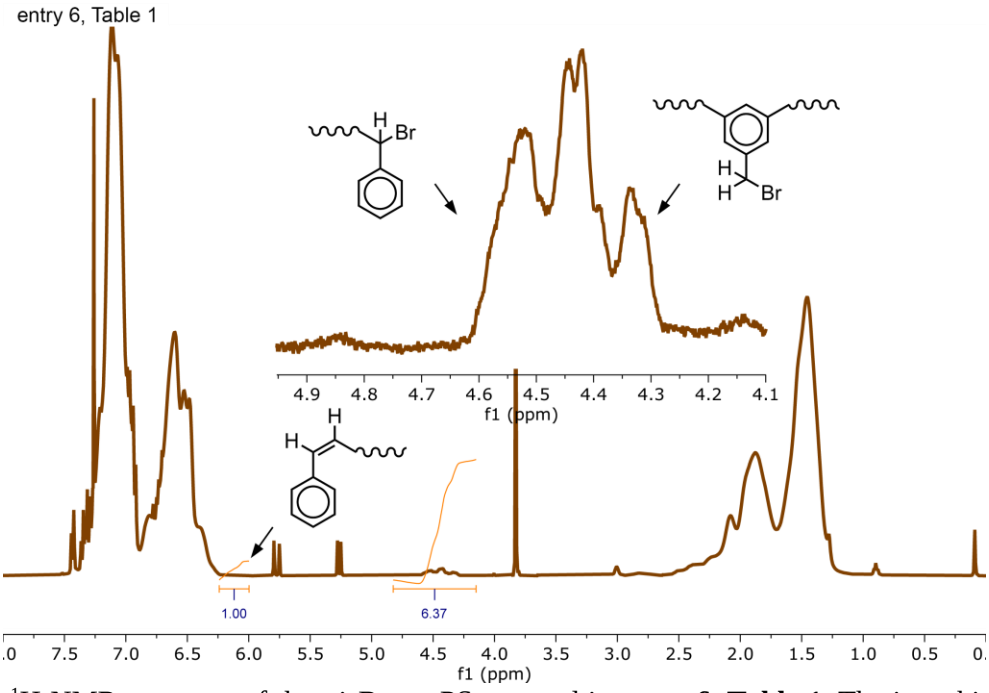

Figure S6. ^{1}H-NMR spectrum of the trisBromoPS reported in **entry 6**, **Table 1**. The inset highlights the proton signals geminal to the bromide functionality. The integrations of the above-mentioned signals and of the dehydrohalogenated chain-ends are given in the spectrum.

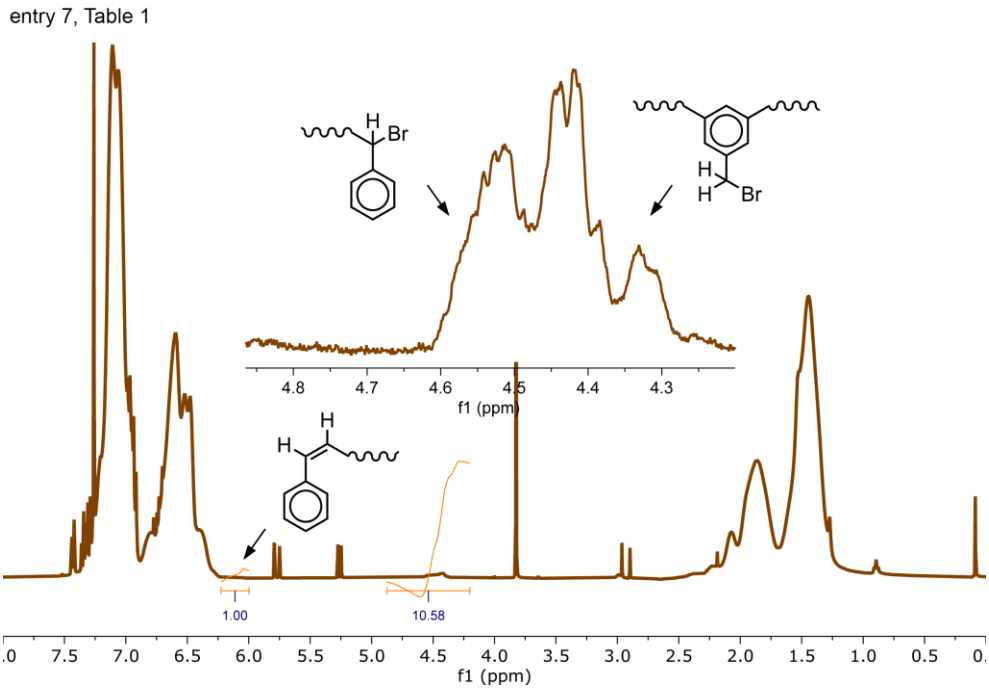

Figure S7. ^{1}H-NMR spectrum of the trisBromoPS reported in **entry 7**, **Table 1**. The inset highlights the proton signals geminal to the bromide functionality. The integration of the above-mentioned signals and of the dehydrohalogenated chain-ends are given in the spectrum.

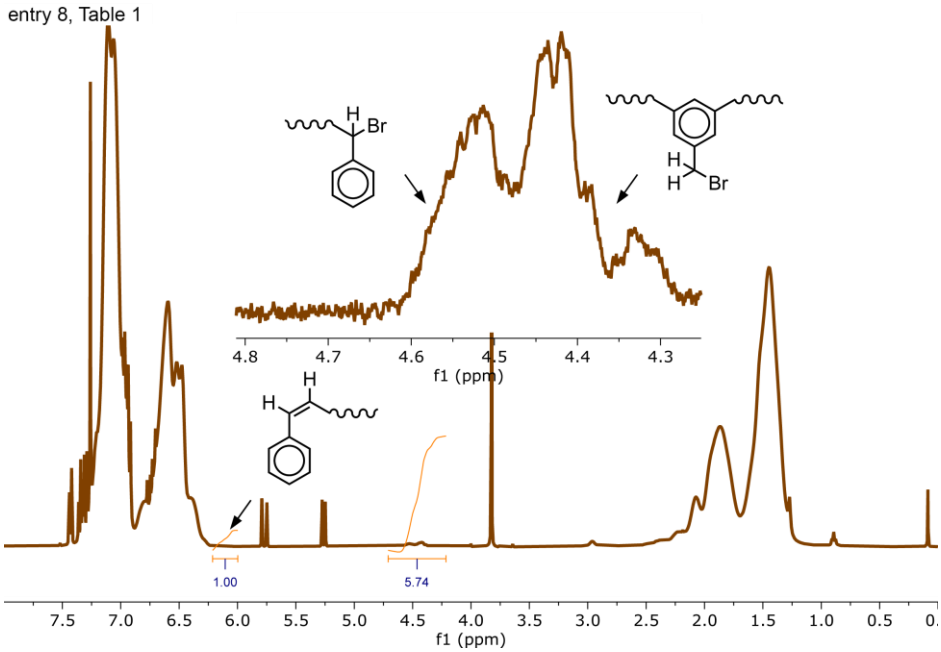

Figure S8. ^{1}H-NMR spectrum of the trisBromoPS reported in **entry 8**, **Table 1**. The inset highlights the proton signals geminal to the bromide functionality. The integration of the above-mentioned signals and of the dehydrohalogenated chain-ends are given in the spectrum.

Table S1. Characterization of trisAzidePSs, synthesized via nucleophilic substitution of sodium azide on trisBromoPSs.[a]

Entry	*Yield* (%)	M_n^{GPC} (kDa)	ΔM_n^{GPC}[b] (%)	*Đ*	*f*	χ_{star} [c]	T_g (°C)
1	87.9	2.22	+ 13.5	1.14	2.76	0.06	56.4
2 [d]	95.1	3.16	+ 2.2	1.15	2.90	0.33	70.2
3 [e]	–	–	–	–	–	–	–
4	95.5	4.39	+ 8.6	1.13	2.91	0.50	78.2
5	95.5	5.90	– 0.2	1.13	2.91	0.61	83.8
6	95.7	7.51	– 0.4	1.13	2.80	0.67	88.6
7	97.5	11.02	+ 2.5	1.14	2.81	0.75	94.3
8	94.9	11.20	– 2.7	1.13	2.81	0.80	94.8

[a] Conditions: sodium azide (1.5 eq. with respect to the bromide functionalities of the trisBromoPS), V_{DMF} = 6 mL/g with respect to $w_{trisBromoPS}$, T = 30 °C, *time* = 4 h.
[b] Calculated as the percent difference with respect to the M_n^{GPC} of the trisBromoPS precursor.
[c] The three-arm star molar fraction (χ_{star}) was calculated as the molar ratio between the ^{1}H-NMR peak assigned to the chain-end PS-CH(Ph)N_3 (δ = 3.8–4.1 ppm) and the peak attributed to the pendant PS-Ph(CH_2N_3)-PS (δ = 4.1–4.2 ppm).
[d] The amounts of reagents and solvents were increased fivefold.
[e] This experiment, based on **entry 3** in **Table 1**, failed, and the results could not be included in the table. Nonetheless, we retained the entry to maintain consistent numbering with the previous table.

.

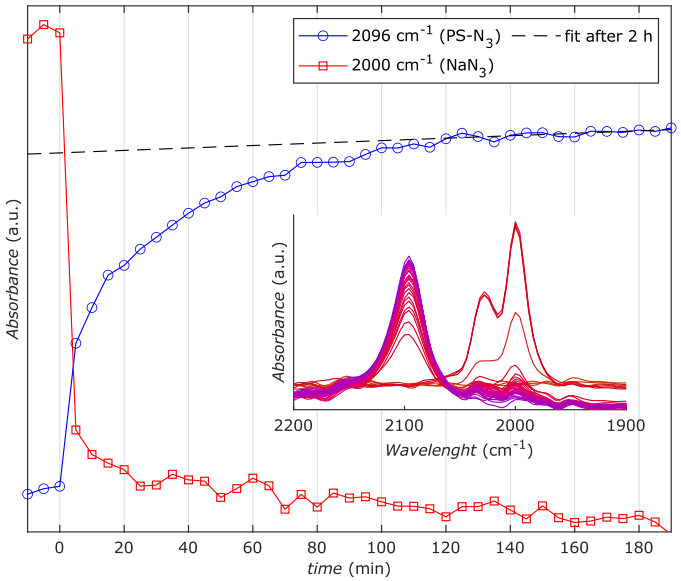

Figure S9. Evolution of the nucleophilic substitution of NaN_3 on trisBromoPS (**entry 1**, **Table S1**) monitored by online ATR FT-IR.. The inset shows the decrease in intensity of the double peak at 2000 cm^{-1} (attributed to NaN_3 dissolved in DMF) as the peak at 2096 cm^{-1} (attributed to azide-functionalized polystyrene) increases in intensity over the course of 3 h. From the spectra the relative values of absorbance were extrapolated and plotted them against the reaction time.

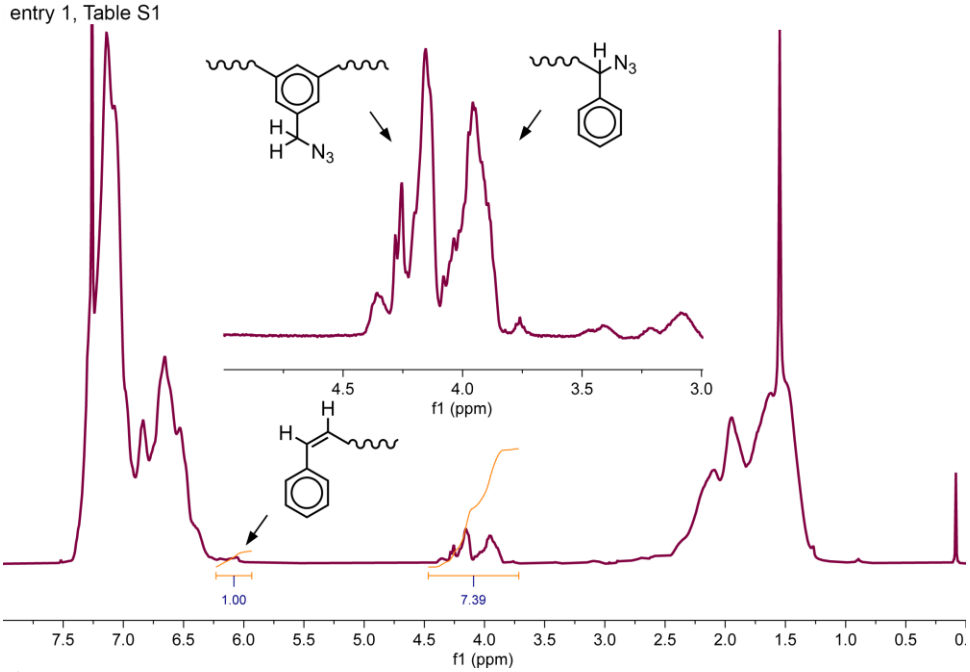

Figure S10. ^{1}H-NMR spectrum of the trisAzidePS reported in **entry 1**, **Table S1**. The inset highlights the proton signals geminal to the azide functionality and the quantitative disappearance of the one related to the brominated precursor. The integrations of the above-mentioned signals and of the dehydrohalogenated chain-ends are given in the spectrum.

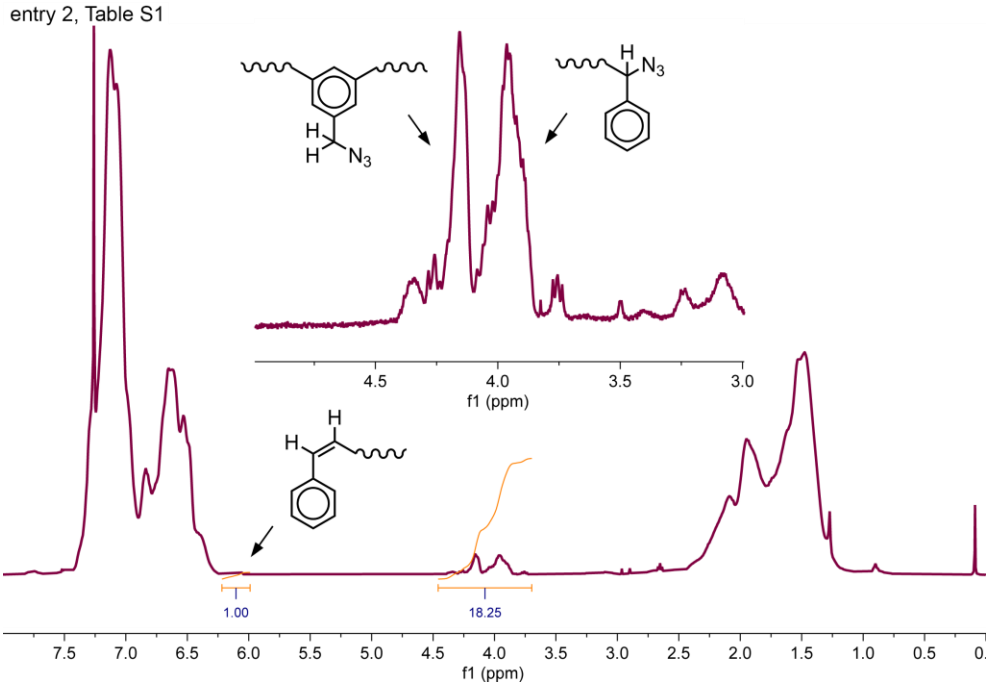

Figure S11. ^{1}H-NMR spectrum of the trisAzidePS reported in **entry 2**, **Table S1**. The inset highlights the proton signals geminal to the azide functionality and the quantitative disappearance of the one related to the brominated precursor. The integrations of the above-mentioned signals and of the dehydrohalogenated chain-ends are given in the spectrum.

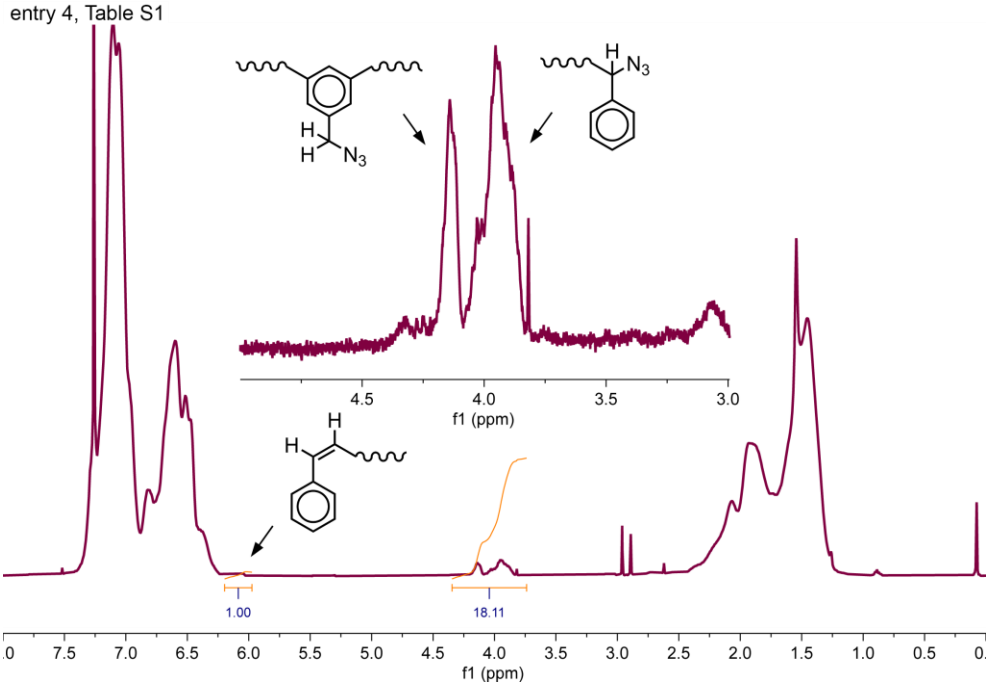

Figure S12. ^{1}H-NMR spectrum of the trisAzidePS reported in **entry 4**, **Table S1**. The inset highlights the proton signals geminal to the azide functionality and the quantitative disappearance of the one related to the brominated precursor. The integrations of the above-mentioned signals and of the dehydrohalogenated chain-ends are given in the spectrum.

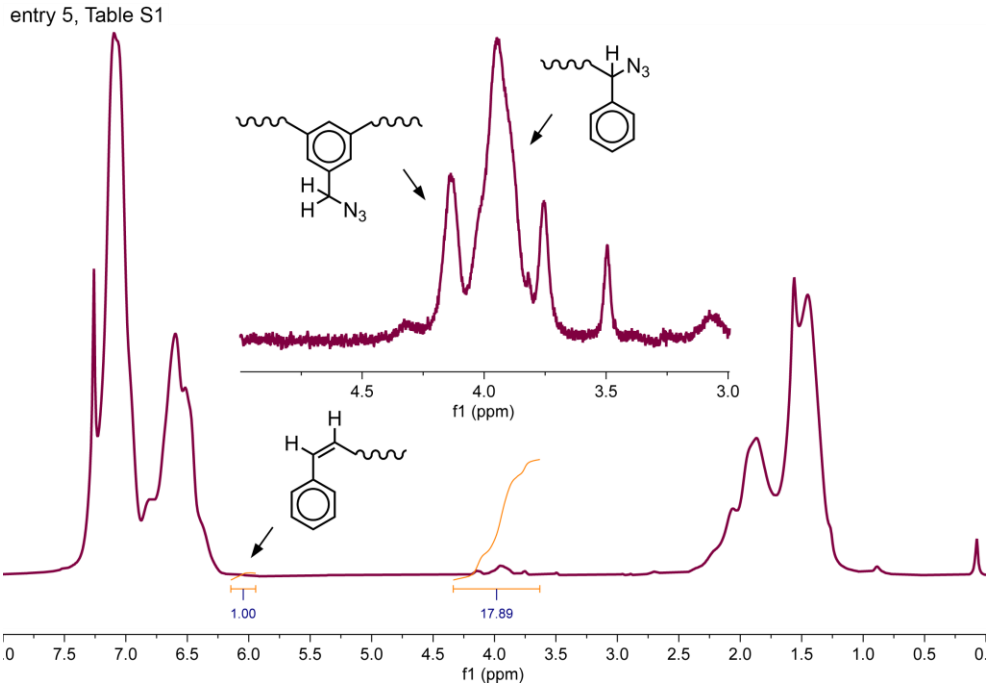

Figure S13. ^{1}H-NMR spectrum of the trisAzidePS reported in **entry 5**, **Table S1**. The inset highlights the proton signals geminal to the azide functionality and the quantitative disappearance of the one related to the brominated precursor. The integrations of the above-mentioned signals and of the dehydrohalogenated chain-ends are given in the spectrum.

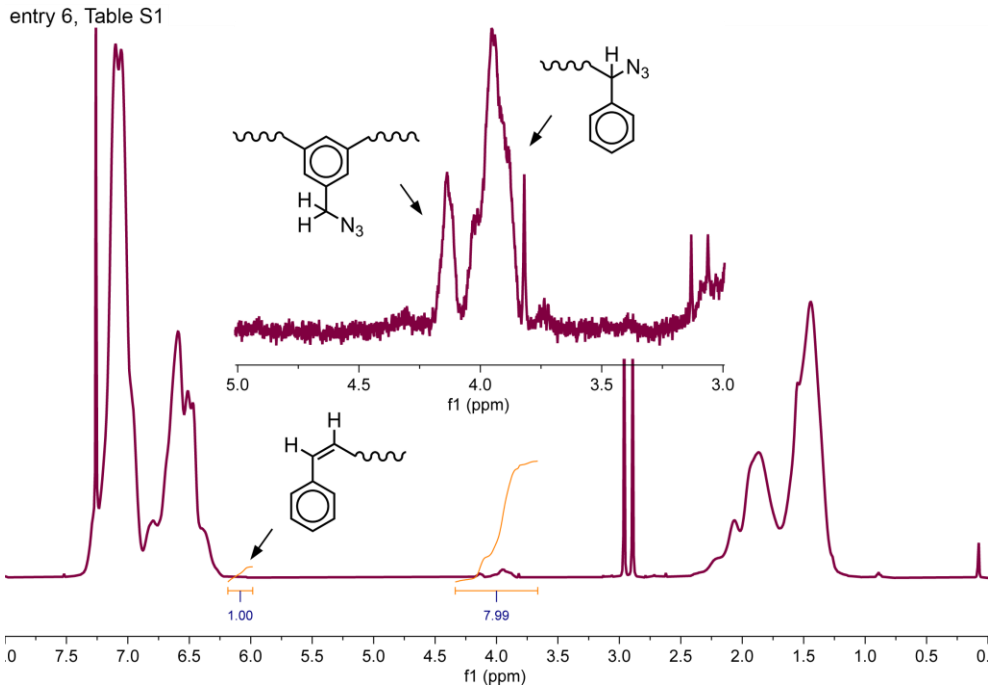

Figure S14. ^{1}H-NMR spectrum of the trisAzidePS reported in **entry 6**, **Table S1**. The inset highlights the proton signals geminal to the azide functionality and the quantitative disappearance of the one related to the brominated precursor. The integrations of the above-mentioned signals and of the dehydrohalogenated chain-ends are given in the spectrum.

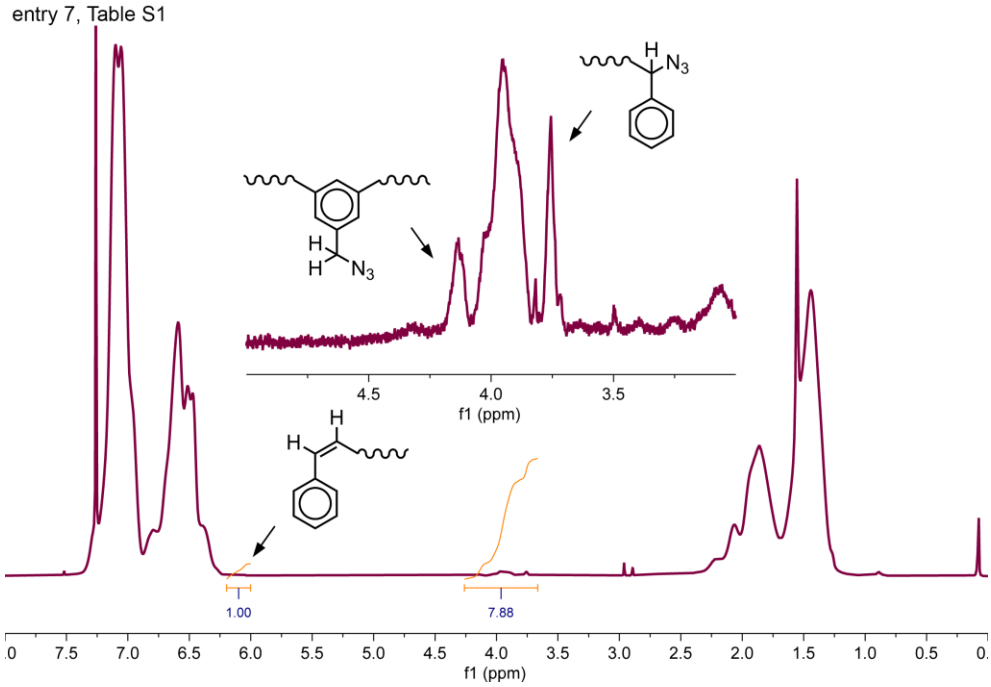

Figure S15. ^{1}H-NMR spectrum of the trisAzidePS reported in **entry 7**, **Table S1**. The inset highlights the proton signals geminal to the azide functionality and the quantitative disappearance of the one related to the brominated precursor. The integrations of the above-mentioned signals and of the dehydrohalogenated chain-ends are given in the spectrum.

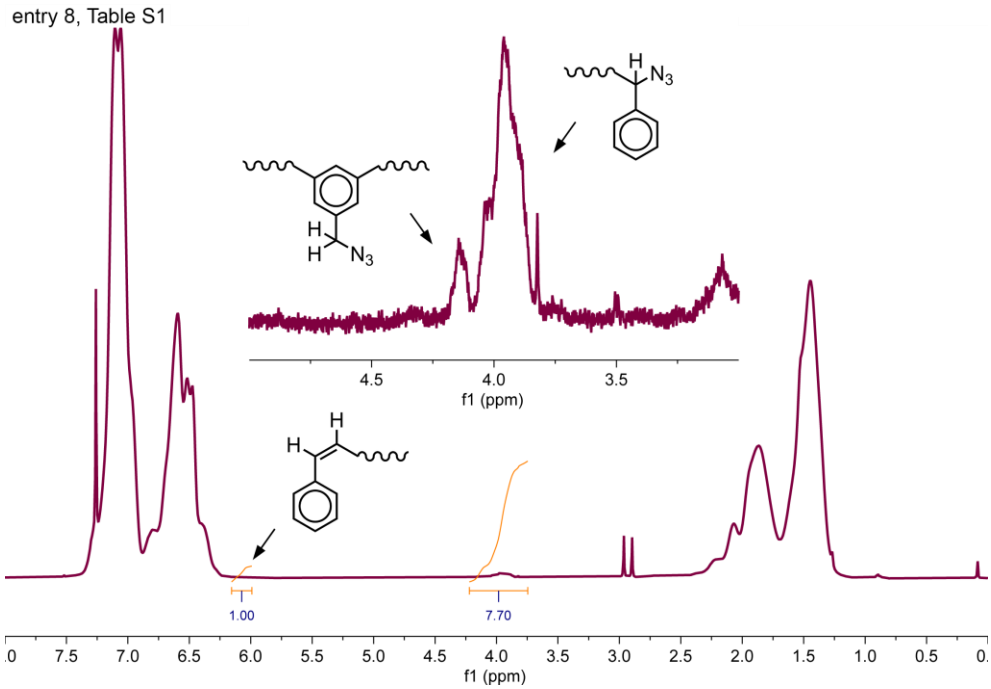

Figure S16. ^{1}H-NMR spectrum of the trisAzidePS reported in **entry 8**, **Table S1**. The inset highlights the proton signals geminal to the azide functionality and the quantitative disappearance of the one related to the brominated precursor. The integrations of the above-mentioned signals and of the dehydrohalogenated chain-ends are given in the spectrum.

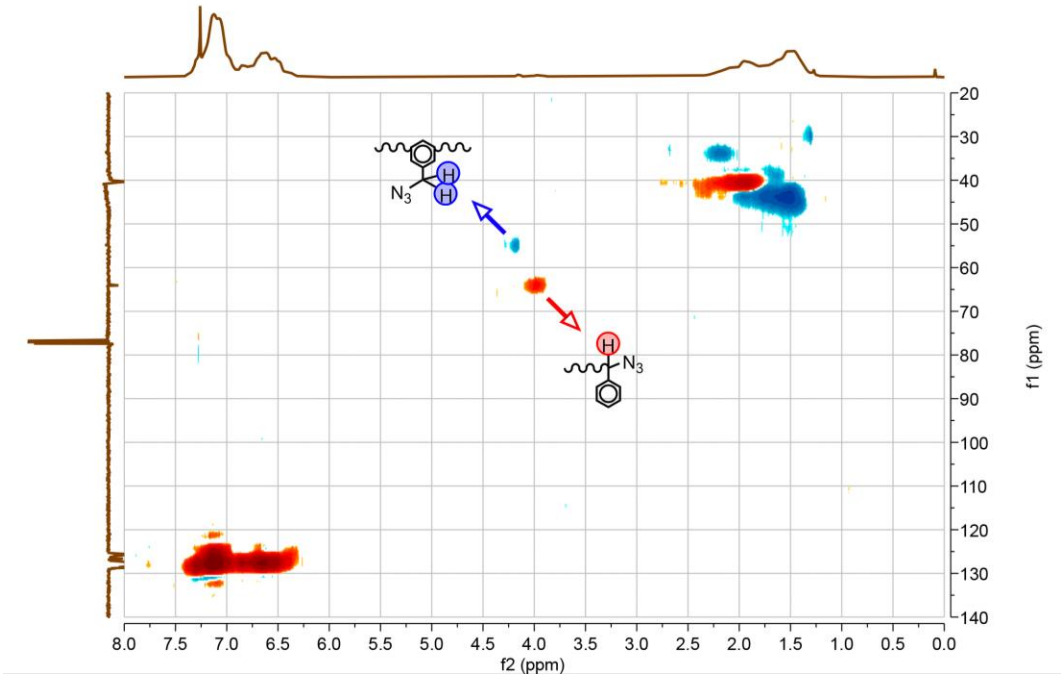

Figure S17. HSQC spectrum of the trisAzidePS (**entry 2**, **Table S1)** with PS-Ph(C**H**$_2$N$_3$)-PS (^{1}H = 4.1-4.2 ppm, ^{13}C = 53-55 ppm, *blue*) and PS-C**H**(Ph)N$_3$ (^{1}H = 3.8-4.1 ppm, ^{13}C = 62-66 ppm *red*).

Table S2. Characterization of trisAminoPSs, synthesized via Staudinger's reaction on trisAzidePSs.[a]

Entry	*yield* (%)	M_n^{GPC} (kDa)	ΔM_n^{GPC}[b] (%)	*Đ*	*f*	T_g (°C)
1	63.9	2.58	+ 15.0	1.13	2.75	71.3
2 [c]	77.9	3.67	+ 14.9	1.15	2.78	79.6
3 [d]	–	–	–	–	–	–
4	97.1	4.69	+ 6.6	1.17	2.80	82.6
5 [e]	90.4	7.46	+ 23.4	1.34	2.82	–
6	98.4	7.94	+ 5.6	1.19	2.78	91.2
7 [e]	98.6	12.18	+ 10.0	1.39	2.84	–
8	98.2	12.62	+ 11.9	1.24	2.76	86.2

[a] Conditions: tributylphosphine (2 eq with respect to the azide functionalities of the trisAzidePS), V_{THF} = 6 mL(/g of trisAzidePS), T = 60 °C, t = 0.5 h. Then, V_{H2O} = 0.6 mL(/g) is added and the mixture stirred at 60 °C overnight.
[b] Calculated as the percent difference with respect to the M_n^{GPC} of the trisAzidePS precursor.
[c] The amounts of reagents and solvents were increased fivefold.
[d] This experiment, based on entry 3 in Table 1, failed but the entry is included for consistent numbering.
[e] Between the addition of tributylphosphine and water, 3 h were waited instead of 0.5 h.

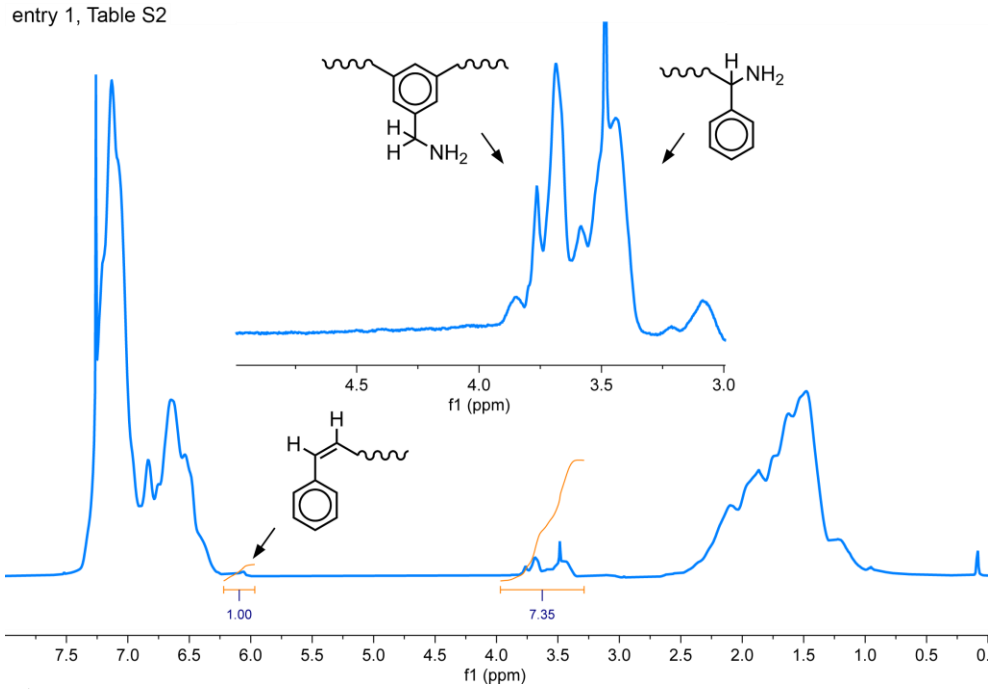

Figure S18. ^{1}H-NMR spectrum of the trisAminoPS reported in **entry 1**, **Table S2**. The inset highlights the proton signals geminal to the amine functionality and the quantitative disappearance of the one related to the azido precursor. The integrations of the above-mentioned signals and of the dehydrohalogenated chain-ends are given in the spectrum.

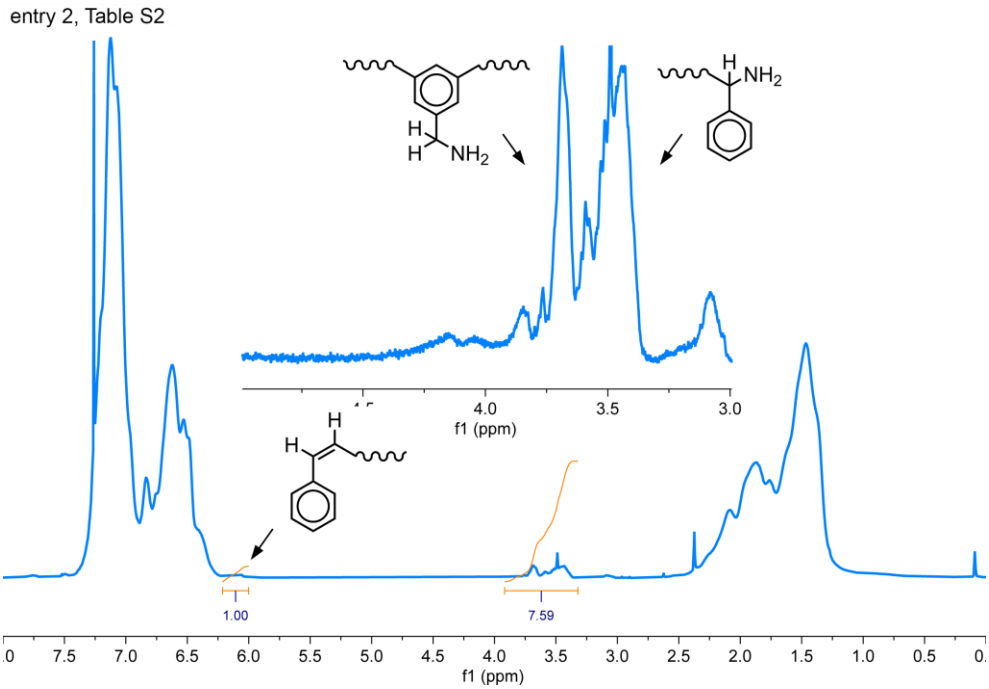

Figure S19. ^{1}H-NMR spectrum of the trisAminoPS reported in **entry 2**, **Table S2**. The inset highlights the proton signals geminal to the amine functionality and the quantitative disappearance of the one related to the azido precursor. The integrations of the above-mentioned signals and of the dehydrohalogenated chain-ends are given in the spectrum.

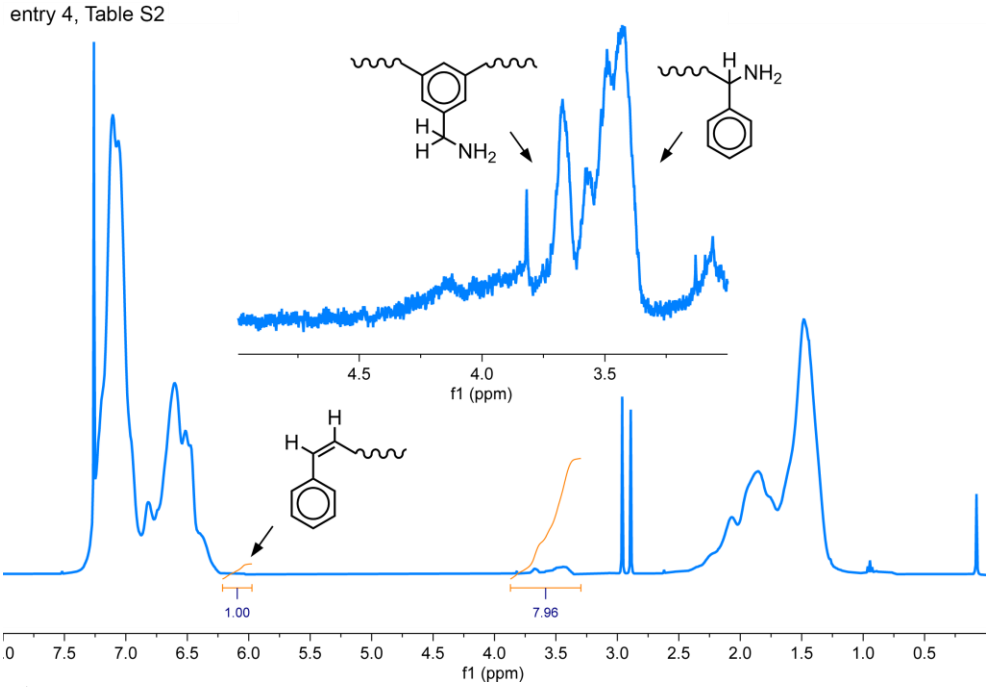

Figure S20. ^{1}H-NMR spectrum of the trisAminoPS reported in **entry 4**, **Table S2**. The inset highlights the proton signals geminal to the amine functionality and the quantitative disappearance of the one related to the azido precursor. The integrations of the above-mentioned signals and of the dehydrohalogenated chain-ends are given in the spectrum.

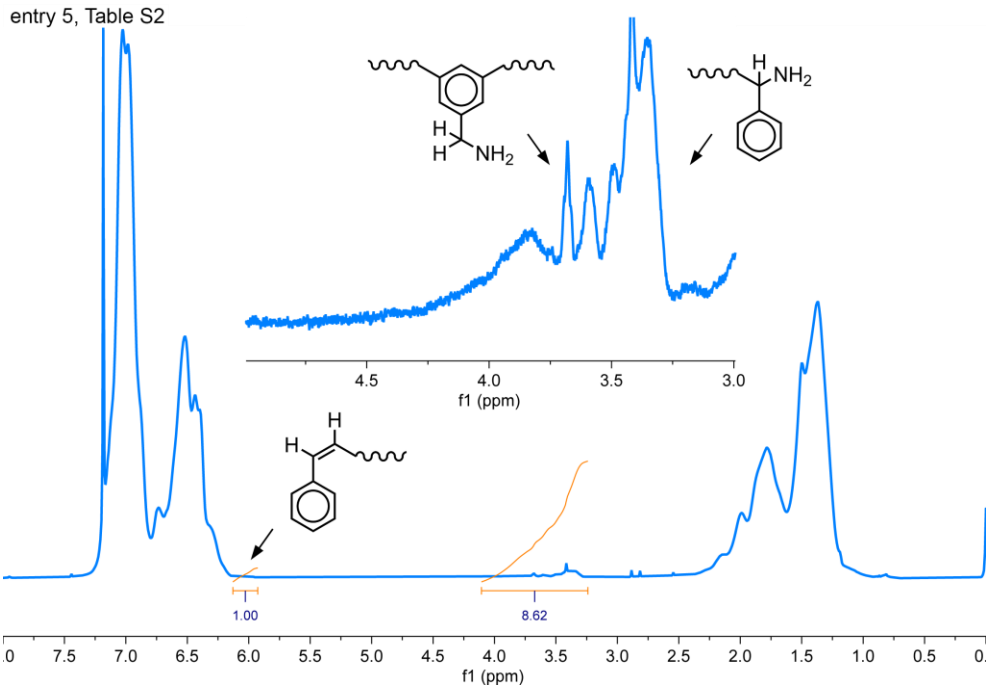

Figure S21. ^{1}H-NMR spectrum of the trisAminoPS reported in **entry 5**, **Table S2**. The inset highlights the proton signals geminal to the amine functionality and the quantitative disappearance of the one related to the azido precursor. The integrations of the above-mentioned signals and of the dehydrohalogenated chain-ends are given in the spectrum.

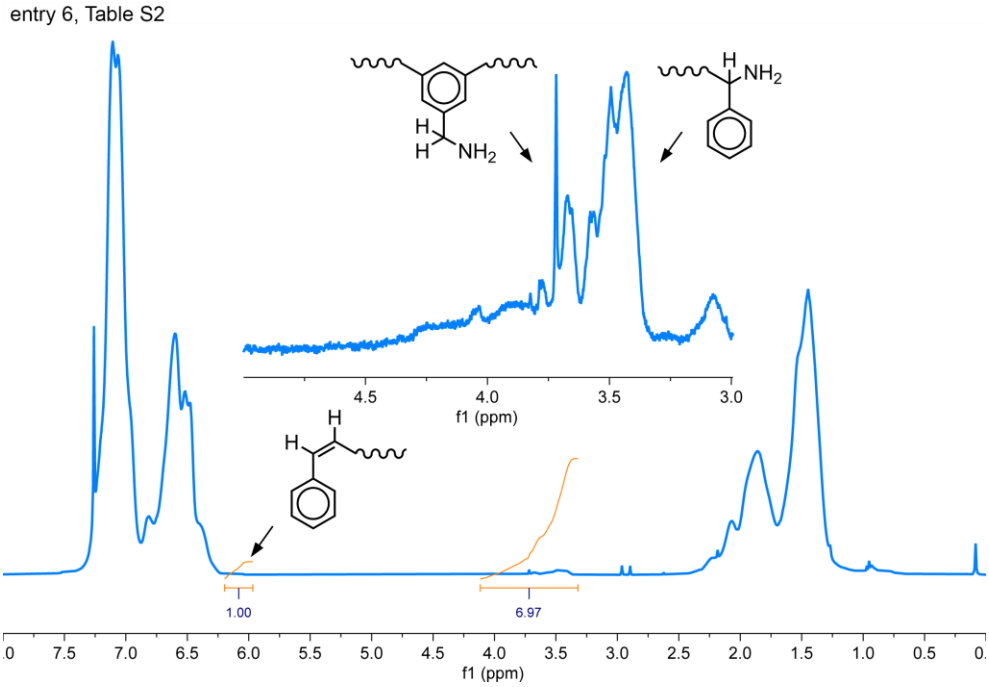

Figure S22. ^{1}H-NMR spectrum of the trisAminoPS reported in **entry 6**, **Table S2**. The inset highlights the proton signals geminal to the amine functionality and the quantitative disappearance of the one related to the azido precursor. The integrations of the above-mentioned signals and of the dehydrohalogenated chain-ends are given in the spectrum.

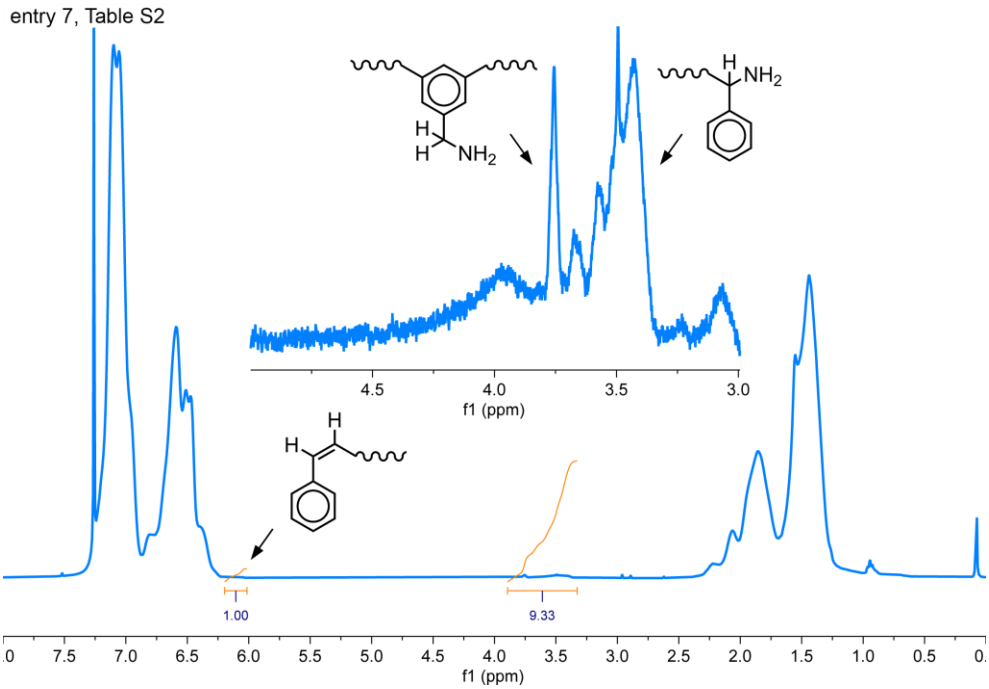

Figure S23. ^{1}H-NMR spectrum of the trisAminoPS reported in **entry 7**, **Table S2**. The inset highlights the proton signals geminal to the amine functionality and the quantitative disappearance of the one related to the azido precursor. The integrations of the above-mentioned signals and of the dehydrohalogenated chain-ends are given in the spectrum.

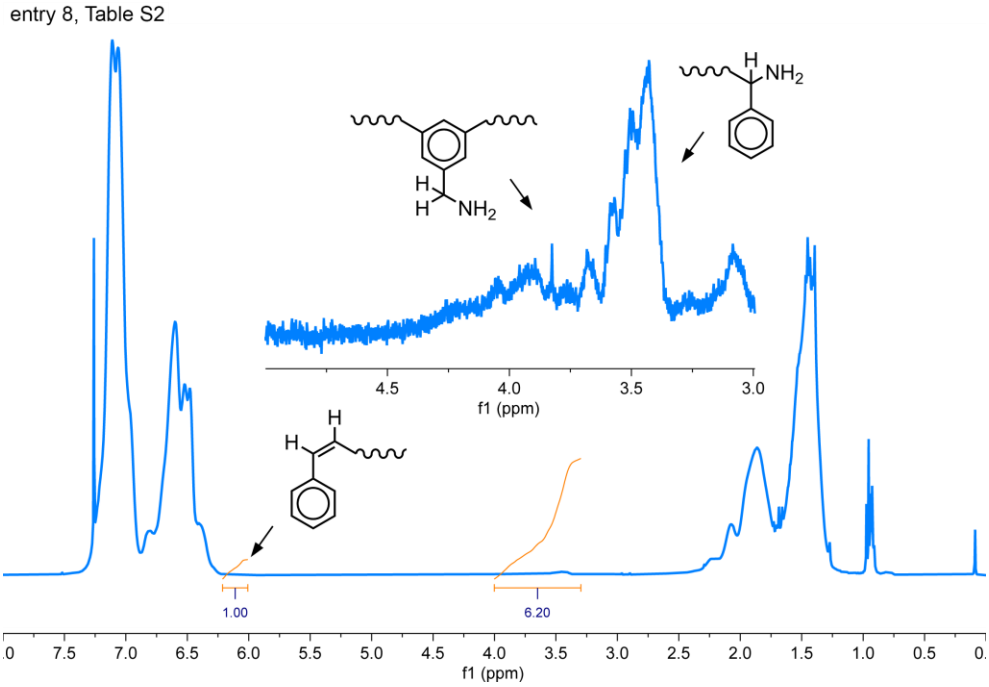

Figure S24. ^{1}H-NMR spectrum of the trisAminoPS reported in **entry 8**, **Table S2**. The inset highlights the proton signals geminal to the amine functionality and the quantitative disappearance of the one related to the azido precursor. The integrations of the above-mentioned signals and of the dehydrohalogenated chain-ends are given in the spectrum.

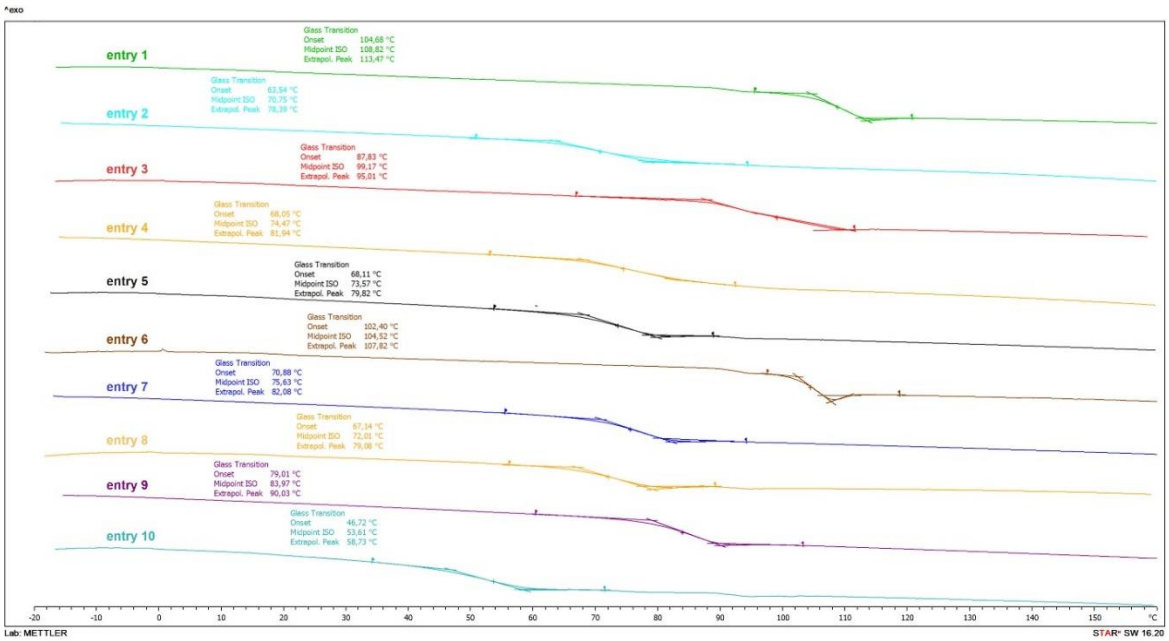

Figure S25. Overlay of DSC traces of the obtained networks, second heating scan (5 °C/min). From **entry 1** to **entry 5 (Table 2)**, epoxy-based networks obtained by reacting BADGE with **trisAminoPS**, from **entry 6** to **entry 10**, vinylogous urethane-based associative CANs obtained by reacting Pripol 2033 acetoacetate with **trisAminoPS**.

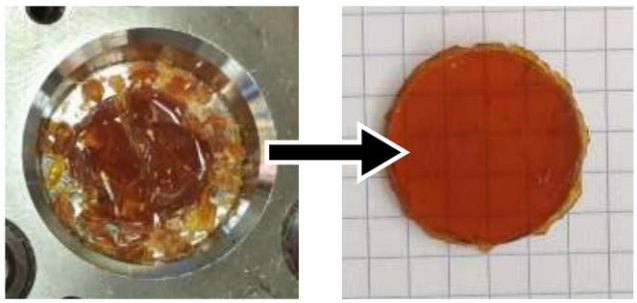

Figure S26. Reprocessing of a vinylogous-urethane network (**entry 7**, **Table 2**). *Left*, broken pieces of the product retrieved after synthesis. *Right*) the reprocessed product after 60 min at 160 °C under 4 metric Ton.

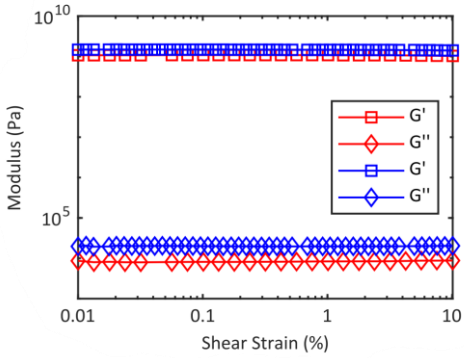

Figure S27. Comparison in amplitude sweep experiments, conducted at 130 °C, between two vinylogous-urethane networks (**entry 7** and **9**, **Table 2**, *blue* and *red*, respectively).

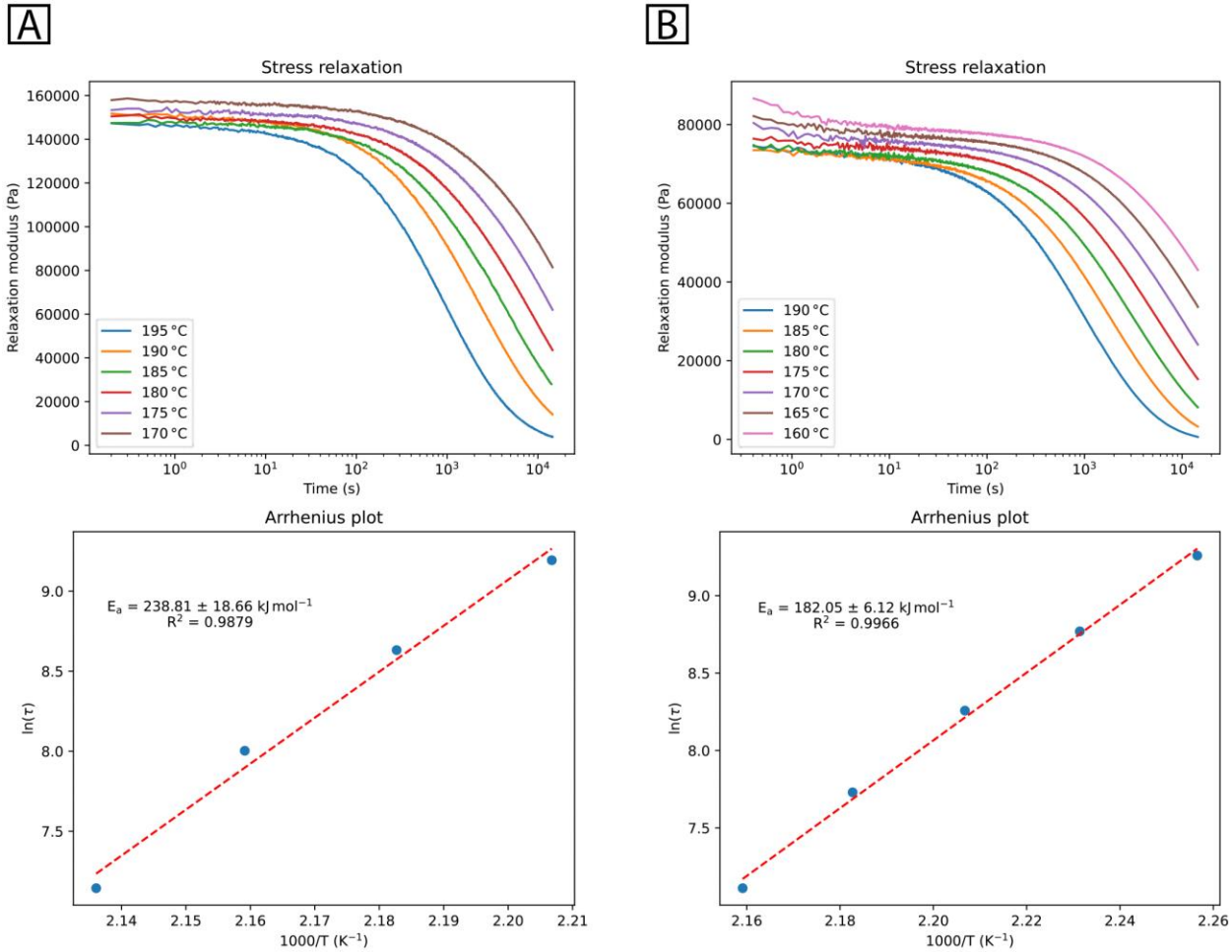

Figure S28. Comparison in stress relaxation experiments between two vinylogous-urethane networks (**entry 7** and **9**, **Table 2**, **A** and **B**, respectively).

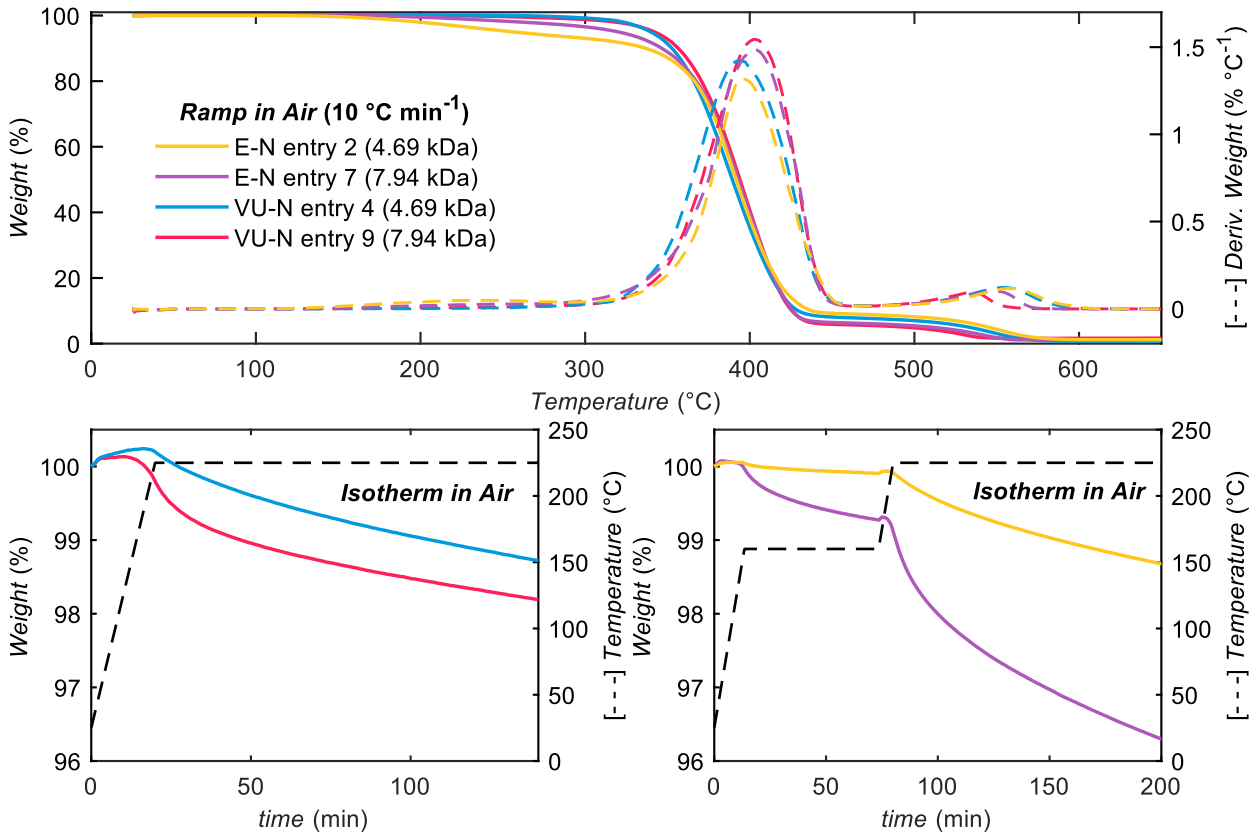

Figure S29. TGA curves of both epoxy and vinylogous urethane networks (E-N and VU-N, respectively). The entries refer to **Table 2** in the manuscript. These analyses were conducted in air.

References:

(1) Gautam, D.; Rao, B. V. Stereoselective Synthesis of (+)-(1R,2S,5S,7R)-2-Hydroxy-Exo-Brevicomin. *Tetrahedron Lett* **2010**, *51* (32), 4199–4201. https://doi.org/10.1016/j.tetlet.2010.06.011.

(2) Denissen, W.; Droesbeke, M.; Nicolaÿ, R.; Leibler, L.; Winne, J. M.; Du Prez, F. E. Chemical Control of the Viscoelastic Properties of Vinylogous Urethane Vitrimers. *Nat Commun* **2017**, *8* (1), 14857. https://doi.org/10.1038/ncomms14857.